Coupling of Power from a Resonant Circuit to Waveguide or Load at Microwave Frequencies

By

Frederick Bernard Wood
B.S. (University of California) 1941

THESIS

Submitted in partial satisfaction of the requirements

for the degree of

MASTER OF SCIENCE

in

Electrical Engineering

in the

GRADUATE DIVISION

of the

UNIVERSITY OF CALIFORNIA

ACKNOWLEDGMENTS

The author wishes to express his appreciation to Professors L. C. Marshall, J. R. Woodyard, D. H. Sloan, W. K. H. Panofsky, and Mr. J. R. Whinnery for their suggestions in connection with this research, to Mr. George A. Becker of the Microwave Laboratory for his assistance in fabricating the resonant cavities, and to Mr. George W. Noller for his assistance in preparing the illustrations.

TABLE OF CONTENTS

LIST OF ILLUSTRATIONS

ABSTRACT

A TM_{020} mode cylindrical resonator similar to one type of resnatron anode resonator in which power is coupled out through a probe-in-resonator to loop-in-waveguide coupling device is investigated. The component parts of the resonator and coupling system are first studied separately and are then combined by joining the equivalent networks corresponding to each component or group of components.

An equation is derived for the theoretical unloaded Q for a cylindrical TM_{020} resonator coupled to a half-wave shorted coaxial line of low characteristic impedance having the same outer radius as the radius of the cylinder. For a theoretical unloaded Q of 3970 for brass at 9030 mc, the experimental results average 3800. Two sections of the cylindrical wall of the resonator are made flat to permit the change of iris width by use of interchangeable plates. The experimental shift in frequency due to this perturbation of the wall is -50 mc., which is within the theoretical outer limit of -130 mc. Experimental curves of loaded Q, coupled Q, and shift in resonant frequency are plotted as functions of iris width.

The theoretical resonant impedance at a probe in the resonator is calculated from E. U. Condon's equation which was derived for small coupling. Experimental tests are

made to see if Condon's equation can be used for large coupling. For probe length equal to half the resonator height, theoretically the voltage standing wave ratio is 78 for iris loading that reduces the unloaded Q to 240, while experimentally the VSWR is 48. The shift in resonant frequency due to the probe is calculated theoretically, by considering the probe as a part of the resonator wall and treating the resonator as a radial transmission line using the equivalent discontinuity capacitances developed by J. R. Whinnery and T. F. Robbins. The experimental resonant frequency stays within ± 50 mc. of theoretical after corrections for shifts due to irises and perturbation of walls are added.

Numerous undesired modes are traced experimentally. The existence of so many other modes is explained by means of a mode chart upon which both coaxial and cylindrical modes are plotted.

The coupling of a 50 ohm coaxial line to 1/2" x 1" waveguide by means of a loop in the waveguide is investigated. An experimental plot of VSWR vs. frequency disclosed three modes near the frequency at which the loop is of quarter-wave length. For one of these modes the resonant VSWR is 4.6. This case departs too far from the conditions for which E. U. Condon's equation for loop coupling was derived to make a simple comparison between theory and experiment.

A loop-in-waveguide to probe-in-resonator coupling is designed by combining the two separate units previously investigated. A TM_{020} resonator with the probe length equal to half the resonator height, for which the resonant VSWR is 40, was joined with a loop in waveguide for which the VSWR is 4.6. Theoretically the VSWR of the combination is 10.4. The experimental resonant VSWR is 11.

I. INTRODUCTION

A. Objective

The object of this investigation is to study the coupling of power to a waveguide from a resonant circuit such as the anode resonator of a resnatron oscillator. The type of resnatron cavity considered is a shape not easily represented by simple mathematical functions, so an approximation shown in figure 1A is used in this study. The test resonator of figure 1A has the walls straightened out to simplify the theoretical treatment. Two coupling irises are provided to load the test resonator in place of the electron beam loading of a resnatron oscillator. The test resonator has been scaled in dimensions to come within the range of available test equipment.

B. Procedure

To study this coupling problem in a way that is of more value in the solution of similar problems, the resonator of figure 1A is broken up into separate parts as shown in figures 1B and 2.

(1) Study of TM_{020} Mode Cylindrical Resonator. Measurements are made of loaded Q and resonant frequency as a function of iris width for a TM_{020} cylindrical resonator with a half-wave shorted coaxial line at the outer radius to correspond to the choke structure of a resnatron. The

coupled Q and shift in resonant frequency are calculated from this data. Numerous references are mentioned in the bibliography.

(2) Study of Probe from Coaxial Line to TM_{020} Resonator. The input impedance, resonant frequency, and other modes of oscillation are investigated.

(a) Condon[2] has derived an equation for the impedance of a probe in a resonator for conditions of small coupling. Experimental measurements are made to see how far Condon's equation is applicable to tight coupling.

(b) If the probe is considered as a part of the resonator, the resonator may be treated as a radial line as described by Ramo and Whinnery.[3]

(c) The interference of other modes is investigated. The reason for the existence of more than the expected TM modes is analyzed.

(3) Study of Loop in Waveguide. Condon's[2] equation for loop coupling for a rectangular resonator is examined to see if it can be used for a resonator that is so heavily loaded that it is essentially non resonant.

(4) Loop in Waveguide to Probe Coupling in TM_{020} Cylindrical Resonator. By use of the theory of microwave coupling systems summarized by Jaynes,[4] resonators of the type shown in figure 1A are designed by appropriate combination of data from parts (1), (2), and (3) above to obtain the desired properties.

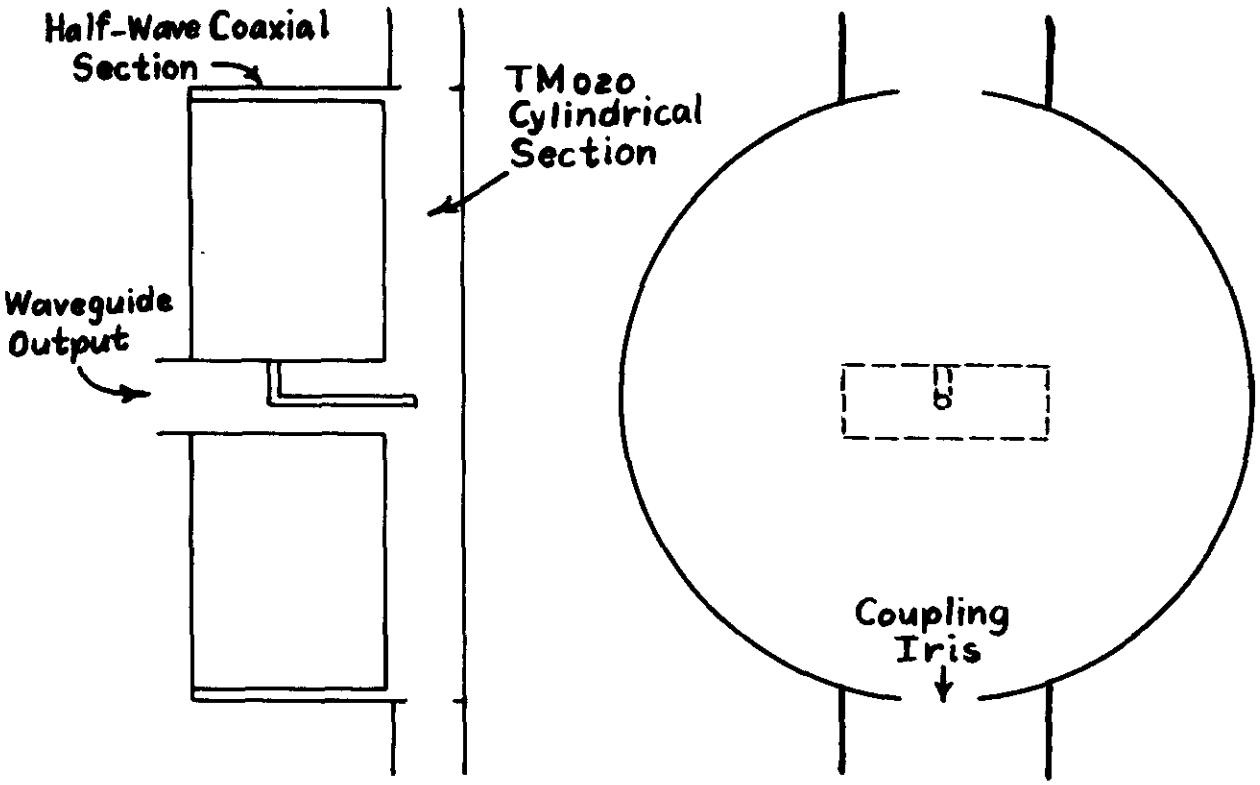

Figure 1A – An Approximation to a Type of Resnatron Anode Resonato

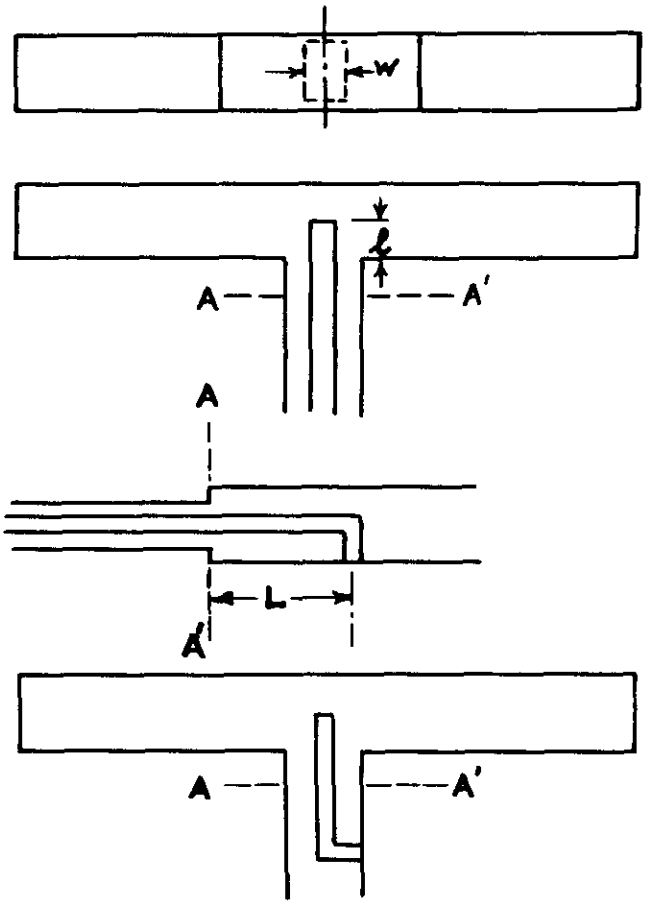

(1) Study of TM020 Resonat as Function of Iris Width.

(2) Study of Probe Couplin from Coaxial Line. Resonator Loaded by Irises of Part (1) to Simulate Electron Bea Loading.

(3) Study of Loop Couplin to Waveguide from Coaxial Line

(4) Combination of Probe and Loop Coupling of Parts (2) and (3).

Figure 1B– Subdivision of the Problem into Component Parts.

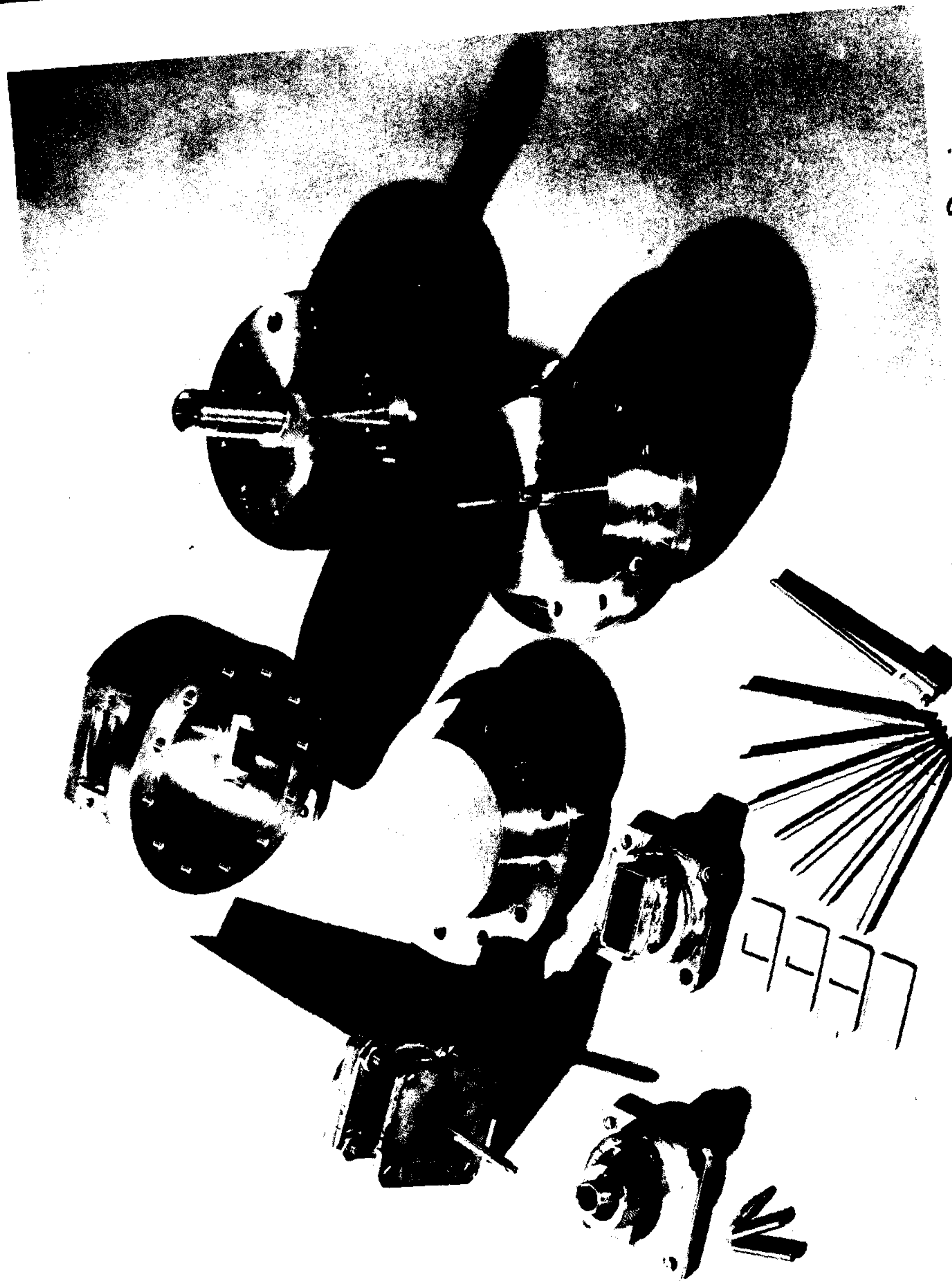

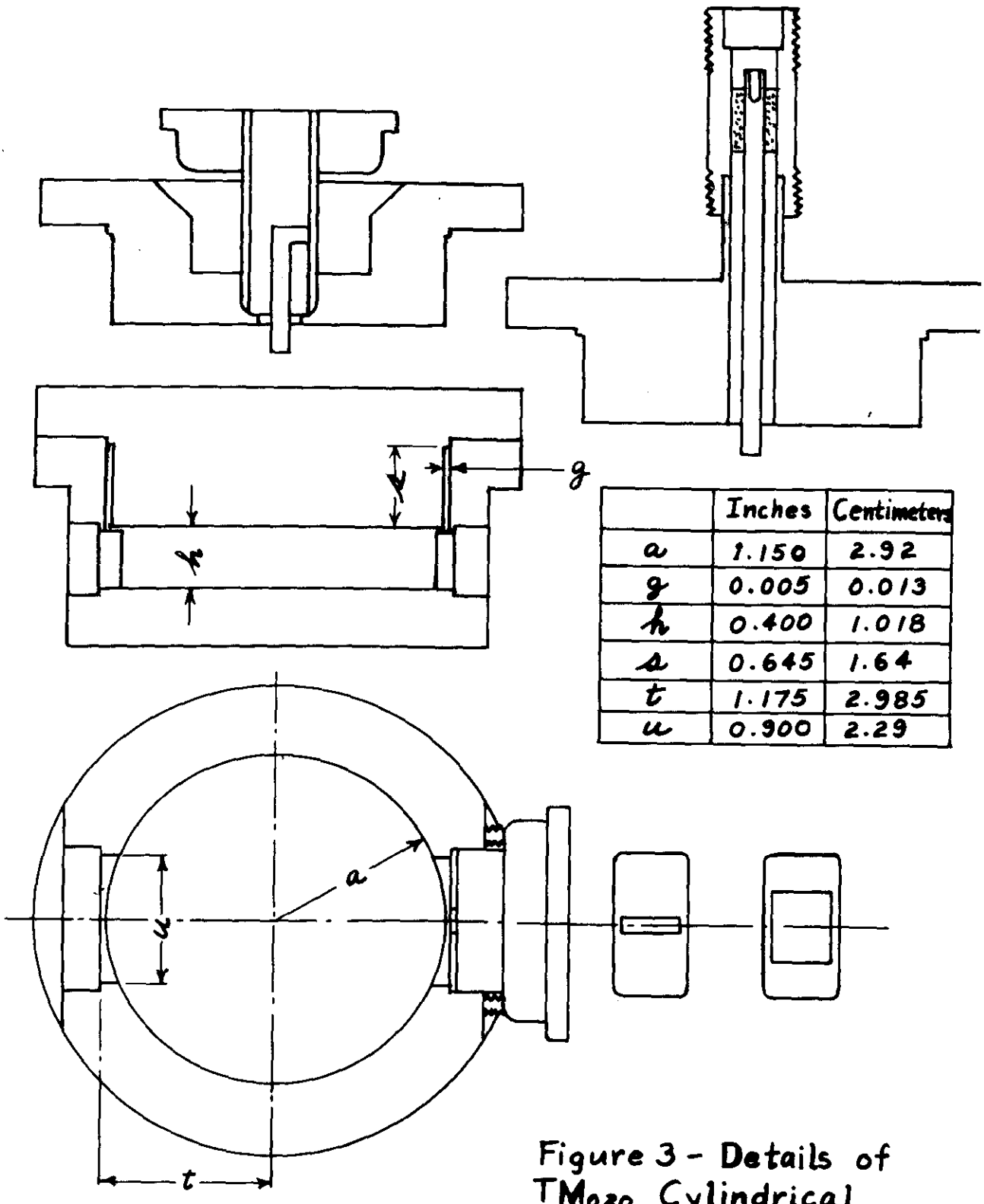

	Inches	Centimeters
a	1.150	2.92
g	0.005	0.013
h	0.400	1.018
s	0.645	1.64
t	1.175	2.985
u	0.900	2.29

Figure 3 - Details of TM_{020} Cylindrical Resonator

II. CYLINDRICAL RESONATOR IN TM_{020} MODE

A. Perfect Cylindrical Resonator

The Q and resonant frequency of the resonator are calculated for a perfect cylinder and are then corrected for the change in Q due to the half-wave coaxial line section and for the change in frequency due to the rectangular bulges at the iris coupling points.

The frequency and unloaded Q of a perfect cylinder having height and radius of resonator of figure 3 for the TM_{020} mode are as follows:

$P_{1n} = P_{02} = k_0 a = \frac{2\pi a}{\lambda_1} = 5.52$, the second root of $J_0(k_c r)$.

$\lambda_1 = \frac{2 \quad 5.52}{5.32} = 3.32$ cm. $\quad f_1 = \frac{c}{\lambda_1} = \frac{3 \times 10^{10}}{3.32} = 9030 \times 10^6$ cycles/sec.

$Q_u = \frac{\eta_1}{R_s} \frac{P_{02}}{2} \frac{1}{1 + \frac{a}{h}} = 7920 \times 2.76 \times 0.258 = 5630$

$\eta_1 = 120$ ohms, characteristic impedance of free space.

$R_s = 5.01 \times 10^{-7} \sqrt{f} = .0476$ ohms/square, the surface resistivity of brass at f = 9030 mc.

B. Cylinder with Half-Wave Coaxial Section Added

At resonance the shorted half-wavelength coaxial line presents zero impedance for the TM_{020} mode at the junction with the wall of the cylindrical resonator, so no change is made in the resonant frequency. The characteristic impedance of the coaxial line is 0.26 ohms so that the impedance remains

close to zero for frequencies near the design frequency.

Since the coaxial section changes the surface area of the resonator without a proportional increase in volume, the Q will be lower.

From appendix B, the change in Q is approximately as follows:

$$\frac{Q'_u}{Q_u} = \frac{a + h}{a + h + s} = 0.706 \qquad (2)$$

$$Q'_u = 0.706 \times 5600 = 3970$$

C. Cylinder With Rectangular Perturbation of Cylinder Wall

Near the coupling irises, flat recesses have been made in the cylindrical walls to simplify the changing of iris width. Since this is equivalent to pushing a section of the wall out at a place where there is a large magnetic field and no electric field, the resonant frequency will be appreciably shifted. The change in Q is probably small, since the volume to surface ratio is not seriously changed.

J. C. Slater[5] has given the following equation for the change in frequency of a resonator in which the boundary is pushed in.

$$\omega^2 = \omega_a^2 \left(1 + \int (H_a^2 - E_a^2)\, dv \right) \qquad (3)$$

$\omega = 2\pi f$, the perturbed frequency

$\omega_a = 2\pi f_a$, the unperturbed frequency of mode a.

H_a is the solenoidal function used in expanding H

I_a is the solenoidal function for I

v is volume.

As developed in appendix B for this case this equation reduces approximately to:

$$\left(\frac{313}{313_a}\right)^2 = 1 - \frac{v}{v_0} = 1 - .03 = 0.97 \qquad (4)$$

where v is the volume of the pushed out section and v_0 is the volume of the perfect cylinder.

$$\frac{313}{313_a} = 0.984 \qquad f = 0.984 \times 9030 = 8900 \text{ mc.}$$

This is probably an over correction, because the electric field is assumed to be zero throughout the pushed out volume while it is precisely zero only at the boundary. The experimental shift in frequency is ~80 mc, which is within the outer limit of ~100 mc. calculated above.

B. Loading with Iris Coupling

Empirical measurements of iris coupling are made for use as (1) loading to simulate loaded Q due to electron beam in reasatron cavity and (2) loading as a means of measuring resonance of modes with high transmission loss by using a large iris and then correcting the results for the shift in f_0 and k due to the iris.

From measurements of loaded Q with different input and output iris widths, the coupled k designated by k_c has been

determined from the following equation:

$$\frac{1}{Q_{L12}} = \frac{1}{Q_{c1}} + \frac{1}{Q_u} + \frac{1}{Q_{c2}} \qquad (5)$$

Q_{c1} is the coupled Q of the input iris, Q_{c2} of the output iris, Q_u the unloaded Q, and Q_{L12} the loaded Q.

For iris widths $w_1 = 1/2"$ and $w_2 = 1/8"$, Q_{L12} is determined by measuring the voltage standing wave ratio (β) and phase and then plotting them on a Smith chart as in figure 4. The impedances of figure 4 are referred to a point of voltage maximum, $0.45\lambda_g$ toward the generator from the outside edge of resonator iris. This treatment corresponds to considering the resonator as a series resonant circuit. From the Q circle the resonant frequency f_0 is found and also f_1 and f_2, the frequencies at which:

$$\frac{|E|}{E_0} = \frac{0}{\sqrt{2}} = .1$$

Then the loaded Q is determined from the following:

$$Q_L = \frac{f_0}{f_1 - f_2} \qquad (6)$$

Where β_1 is the β at resonance,

$$Q_{L2} = (1 + \beta_1)Q_{L12} \qquad (7)$$

where β_1 is less than one if $Q_{L2} < Q_{c1}$, and

$$Q_{c1} = \frac{Q_{L2}}{\beta_1} \qquad (8)$$

Sample calculations from figure 4 are as follows:

$$Q_{L12} = \frac{8902}{3920 - 3883} = 241 \qquad Q_{12} = (1 + 11.2)\ 241 = 2941$$

$$Q_{o1} = \frac{2940}{11.2} = 263$$

Q_{L12} is measured by the transmission method in which f_1 and f_2 are the half power points, for various combinations of input and output iris widths. Some are checked by impedance measurements as in figure 4.

Then the various coupled Q's were computed using equation (5). The averaged values for Q_{L1}, Q_o and the shift in frequency (δF) are plotted in figure 5. Some of the variation in the Q values may be due to the interchangeable coupling units not making good contacts in all the tests.

The results of figure 5 have not been compared precisely with the theory. For a theoretical analysis of iris coupling, the work of Bethe, Marshak, and Schwinger should be consulted.[6] Much engineering information on loop, iris, and probe couplings for TR boxes is included in Volume 14 of the MIT Radiation Laboratory Series.[7]

THE EMELOID CO., INC.
ARLINGTON, N. J.
JANUARY 1945

IMPEDANCE (WAVEGUIDE)

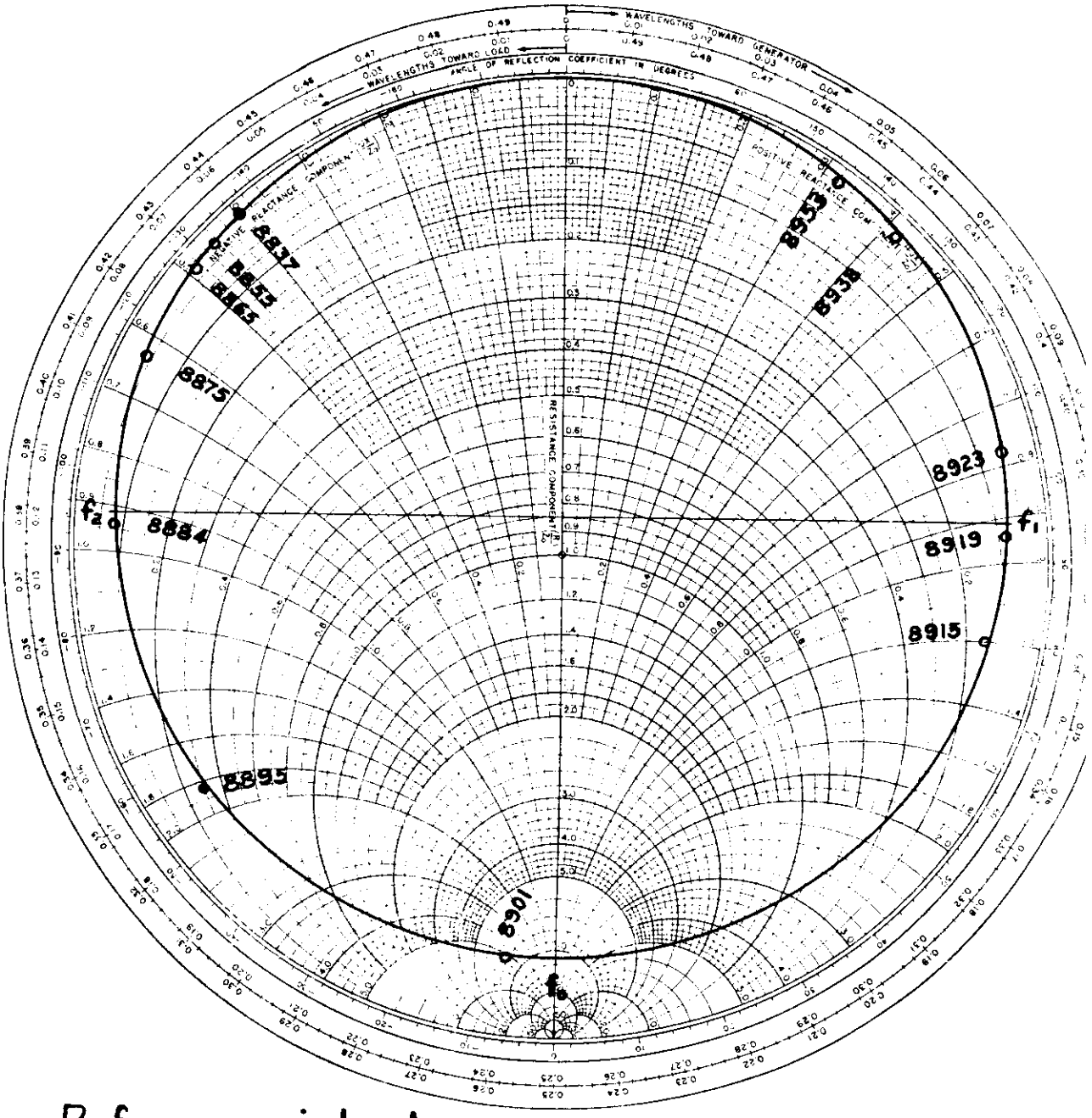

Reference point at
0.45 λ_g toward generator from iris edge.

Ref: Phillip H. Smith "Transmission Line Calculator" Electronics Jan. 1939 and Jan. 1944

Printed in U.S.A.

Figure 4 - Q Circle for TM_{020} Cylindrical Resonator with $\frac{1}{2}$" Input and $\frac{1}{8}$" Output Iris Widths

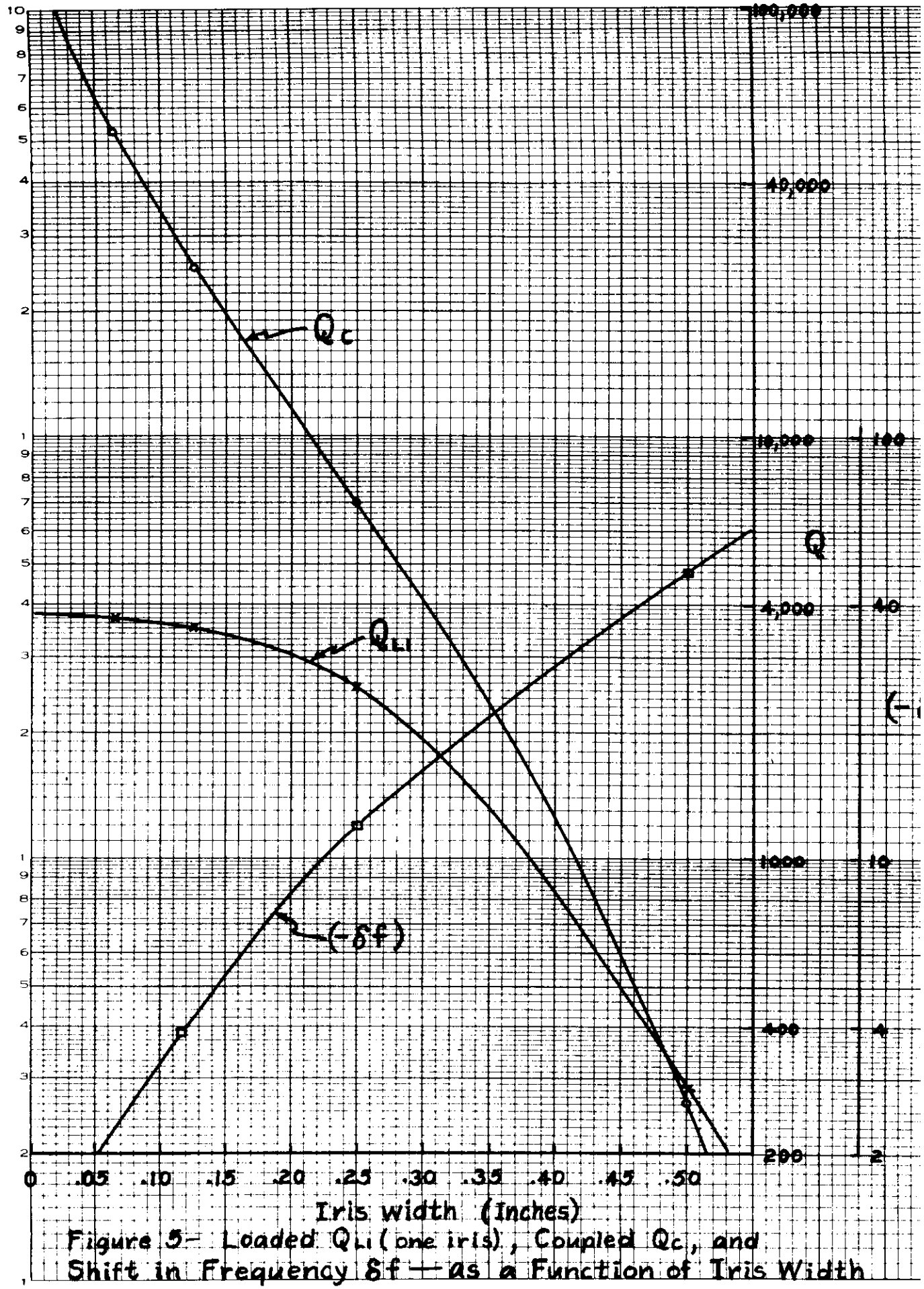

Figure 5- Loaded Q_{L1} (one iris), Coupled Q_c, and Shift in Frequency δf — as a Function of Iris Width

III. Coaxial Line to Probe Coupling in TM_{020} Cylindrical Resonator

A. Considering Resonator as Perfect Cylinder with the Probe Treated as a Coupling Device. (Contrasted to considering the probe as part of cavity, in which case the coupling device is the ring shape iris at base of probe).

This treatment supplies information on the impedance of the resonator seen through a coaxial line at the probe. Condon[2] has developed the following equation for the input impedance of a resonant cavity for probe coupling.

$$Z = 10^{-9}\left[\frac{c^2}{2\pi i f C} + \sum \frac{2\pi i f M_a^2}{\frac{\pi V}{c^2}\left(f_a^2 - f^2 + i\frac{f f_a}{Q_a}\right)}\right] \text{ ohms} \qquad \begin{matrix}(9)\\ \text{c.g.s.}\end{matrix}$$

Where the mutual inductance is:

$$M_a = \int A \cdot ds = \iint \text{curl } A_a \cdot dS \qquad (10)$$

Where V is the volume of the resonator, the magnetic vector potential is normalized as follows:

$$\int A_a(r) \cdot A_b(r)\, dV = \begin{cases} 0 & \text{for } a \neq b \\ V & \text{for } a = b \end{cases} \qquad (11)$$

For the TM_{020} mode at resonance the principal terms of equation (9) are as developed in Appendix C.

$$Z = R + iX$$

$$X = -\frac{1}{\omega C} \text{ ohms}$$

$$R = \frac{36 \times 10^9\ h\ Q}{\omega_a a^2 J_1^2(k_0 a)}\left(\frac{1}{h}\right)^2 \text{ ohms} \qquad \begin{matrix}(12)\\ \text{M.K.S.}\end{matrix}$$

For $(\frac{\ell}{h}) = 1.0$, R is the shunt impedance at the center of the resonator as shown in Appendix D.

For the resonator of figure 3 and $Q_u' = 3970$ the resistive component of impedance at resonance is:

$$R = 250{,}000\ (\frac{\ell}{h})^2 \text{ ohms.} \tag{13}$$

The electrostatic capacitance of the probe can be approximated by considering it as two capacitances in parallel, with a correction factor added for fringing. C_1 is the parallel plate capacitance of the end of the probe and end plate of resonator, and C_2 is the coaxial cylinder capacitance of the probe and outer cylindrical surface of resonator.

For this resonator:

$$C_1 = \epsilon_1 \frac{\pi d^2}{4(h - \ell)} = 0.0277 \left(\frac{1}{1 - \frac{\ell}{h}} \right) 10^{-12} \text{ farads}$$

$$C_2 = \frac{2\pi\epsilon_1}{\ln \frac{2a}{d}} \ell = 0.194\ (\frac{\ell}{h})\ 10^{-12} \text{ farads} \tag{14}$$

M.K.S.

Using an approximate factor of 1.5 to allow for fringing,

$$C = 1.5\ (C_1 + C_2).$$
$$X_L = \frac{-1}{2\pi fC} \tag{16}$$

The resonant impedance, $Z = R + j X_L$, is plotted in figure 6 as a function of probe length.

Figure 6– Input Impedance at 1/8" Diameter Probe in TM_{020} Resonator as Function of Probe Length.

The resonant impedance (R) at the probe as given by equation (13) is too high to measure with the fifty ohm slotted section and probe and the available amplifiers. Equation (12) can be checked experimentally, if the Q is low enough to make β_1 less than 100. The Q can be reduced by making a flatter cavity. However, this would require greater accuracy in the mounting of the probe. A compromise is made by keeping the same cavity height and loading the cavity with two symmetrically placed irises which reduce the Q so that R is within range of the test equipment. This loading is roughly equivalent to the loading of a resnatron cavity by the electron beam.

Loading the resonator with a 1/2" iris to attenuator and crystal on one side and 1/4" iris to matched load on opposite side brings the Q down to 240.

$$R = 15{,}600 \left(\frac{l}{h}\right)^2 \text{ ohms} \quad \text{for } Q_{12} = 240$$

$$\text{For } \frac{l}{h} = 0.5 \quad R = 3{,}910 \text{ ohms.} \tag{17}$$

Using a 50 ohm coaxial slotted section, the theoretical β is:

$$\beta_1 = \frac{3910}{50} = 78$$

Experimentally β_1 was found to be 48, which is approximately two thirds of the theoretical value. An examination of figure 4 shows that if 0.1 $\left(\frac{l}{h}\right)$ is subtracted

from ℓ/h and the inductive reactance due to the terms of equation (9) which were neglected in the approximation of equation (12) are added to the impedance, the experiment and theory would agree very closely for $\ell/h < 0.5$.

Since the theory is derived for a probe of thin cross section and of short length, while in this case we have an 1/8" diameter probe, which goes half way across the resonator, precise agreement would not be expected. This could be investigated in more detail by making a flux plot, by mathematical methods[8] or by a network analyzer method.[9]

The Q-circle for the TM_{020} mode for $\frac{\ell}{h} = 0.5$ is shown in figure 7. Mode A is the desired TM_{020} mode, while Mode B which is also shown in figure 7 is an undesired mode. The impedance looking into the cavity is too high for direct coupling of power into a waveguide or coaxial line, so a transformer must be designed.

B. Considering Resonator as Radial Line

The approach of Section III-A yielded information on the input impedance, but did not supply the shift in resonant frequency due to the loading of the probe. Treatment as a radial line is an easy method of determining the resonant frequencies of TM_{0m0} resonators as described by Hamo and Whinnery.[3]

IMPEDANCE IN COAXIAL LINE (50 OHM)

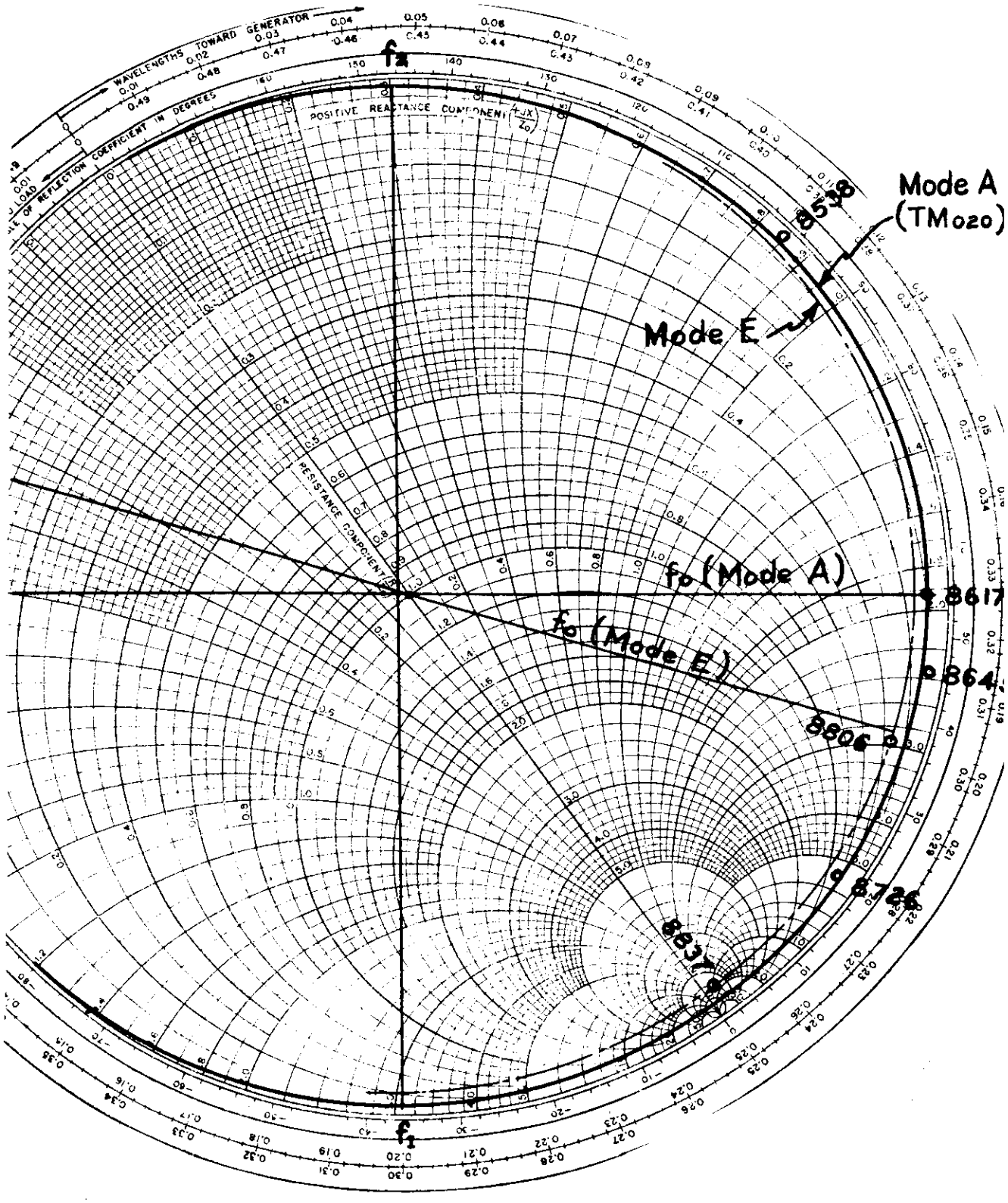

Figure 7- Q Circle for TM020 Cylindrical Resonator with Probe Length Equal to Half of Resonator Height

The resonator is divided into regions A and B as shown in figure 3. Y_{IAT} is the admittance looking toward the center of region A. Y_{IBT} is the admittance looking toward the outer diameter of region B. Y_d is the admittance of the equivalent discontinuity capacitance at the junction of regions A and B. Approximate values of the discontinuity capacitance can be obtained from Whinnery and Jamieson.[10] In this investigation the capacitances have been taken from an unpublished extension to the radial line case by Whinnery and Robbins.[11]

Resonance is determined by the equation:

$$Y_{IAT} + Y_{IBT} + Y_d = 0 \qquad (18)$$

These functions are plotted as functions of frequency in figure 8 for graphical solution of the resonant frequency with different probe lengths.

The results of figure 8 are plotted in figure 9 for comparison with experimental results. The experimental tests were made with 1/2" and 1/4" irises. From figure 5 this gives a shift in frequency of -60 mc. for a perfect cylinder. The probe distorts the fields so that the current at the irises decreases with increased length of probe, so the effect of the irises decreases with probe length. An additional shift in frequency is caused by the pushed out walls near the iris described in Section II C.

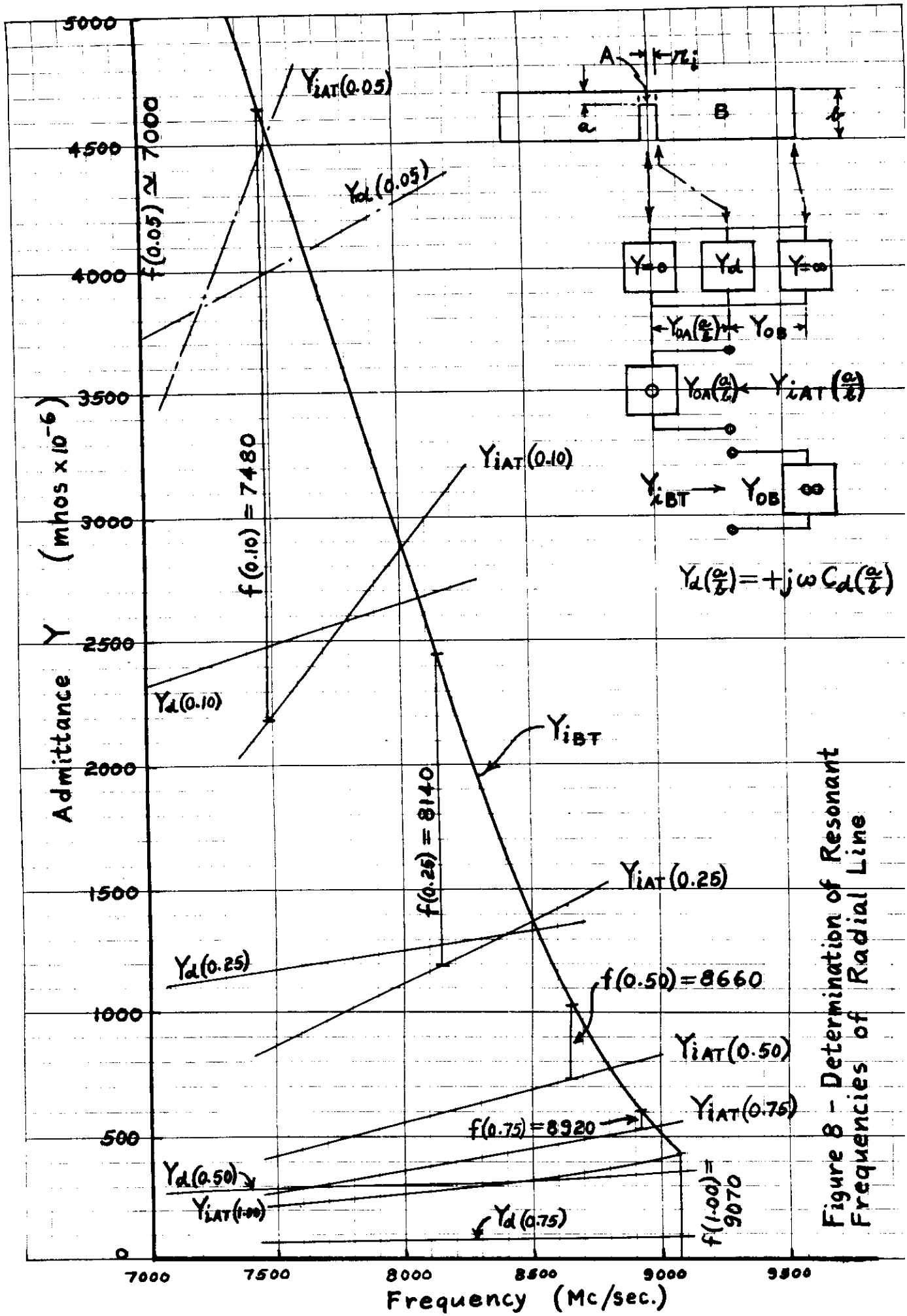

Figure 8 - Determination of Resonant Frequencies of Radial Line

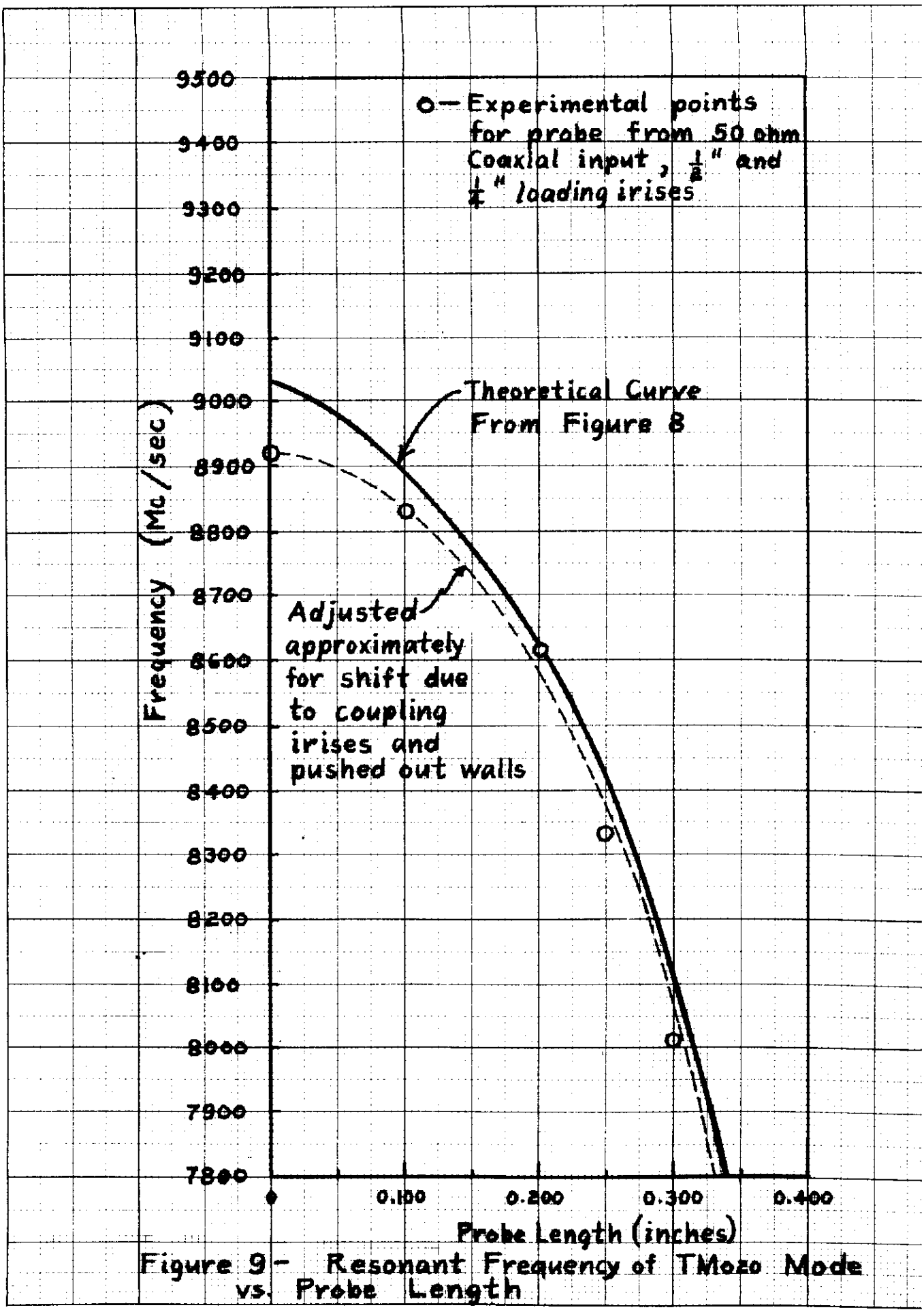

Figure 9 - Resonant Frequency of TM020 Mode vs. Probe Length

C. Interference of Undesired Modes

To see what modes may interfere, a mode chart is prepared in the form used by Kinzer.[12] Perfect cylindrical modes are designated c^{TE}_{lmn}, c^{TM}_{lmn}. Perfect coaxial modes are designated x^{TE}_{lmn}, x^{TM}_{lmn}. Barrow and Mieher[15] have shown what happens to the resonant frequency of the modes near the TM_{010} mode as a cylindrical resonator is changed to a coaxial resonator. Their results for c^{TM}_{010} mode are indicated in figure 10 by points c and d for comparison.

In the present case (TM_{020}) the value of $\frac{D}{L}$ is chosen to put the resonator in a place on the mode chart that will be relatively free of other modes, except that the effect of probe coupling is neglected. The insertion of a center probe changes the electrical length of the resonator for resonance (as far as n > o modes are concerned) from $\frac{\lambda g}{2}$ to approximately $\frac{\lambda}{4}$ or $\frac{\lambda g}{4}$ so that the equivalent length is multiplied by two, so that modes in the region near $1/4\ (\frac{D}{L})^2$ can be encountered. In figure 10 this is illustrated by the line from point a to b.

The modes found experimentally in the TM_{020} resonator are shown in figure 11.

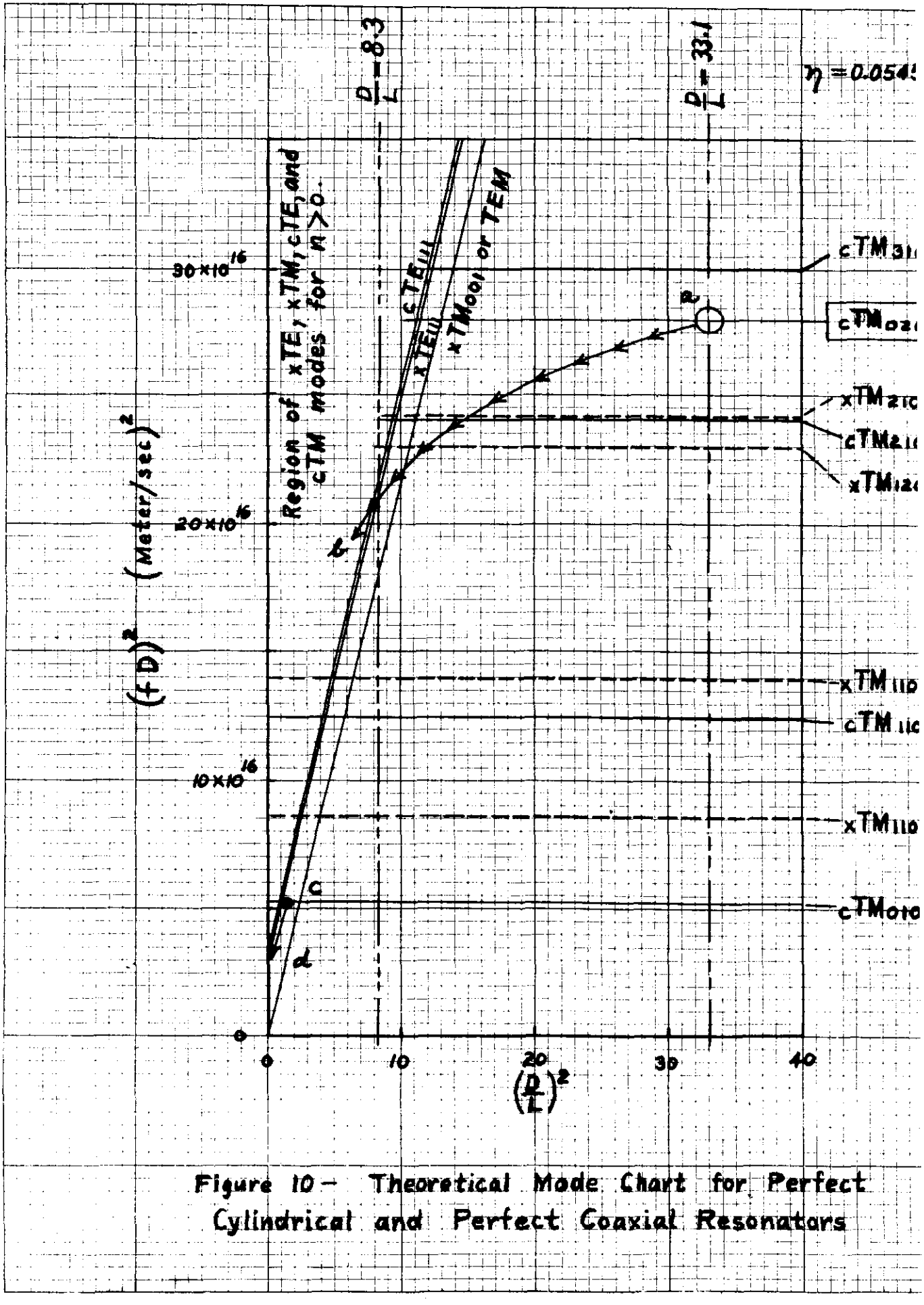

Figure 10 – Theoretical Mode Chart for Perfect Cylindrical and Perfect Coaxial Resonators

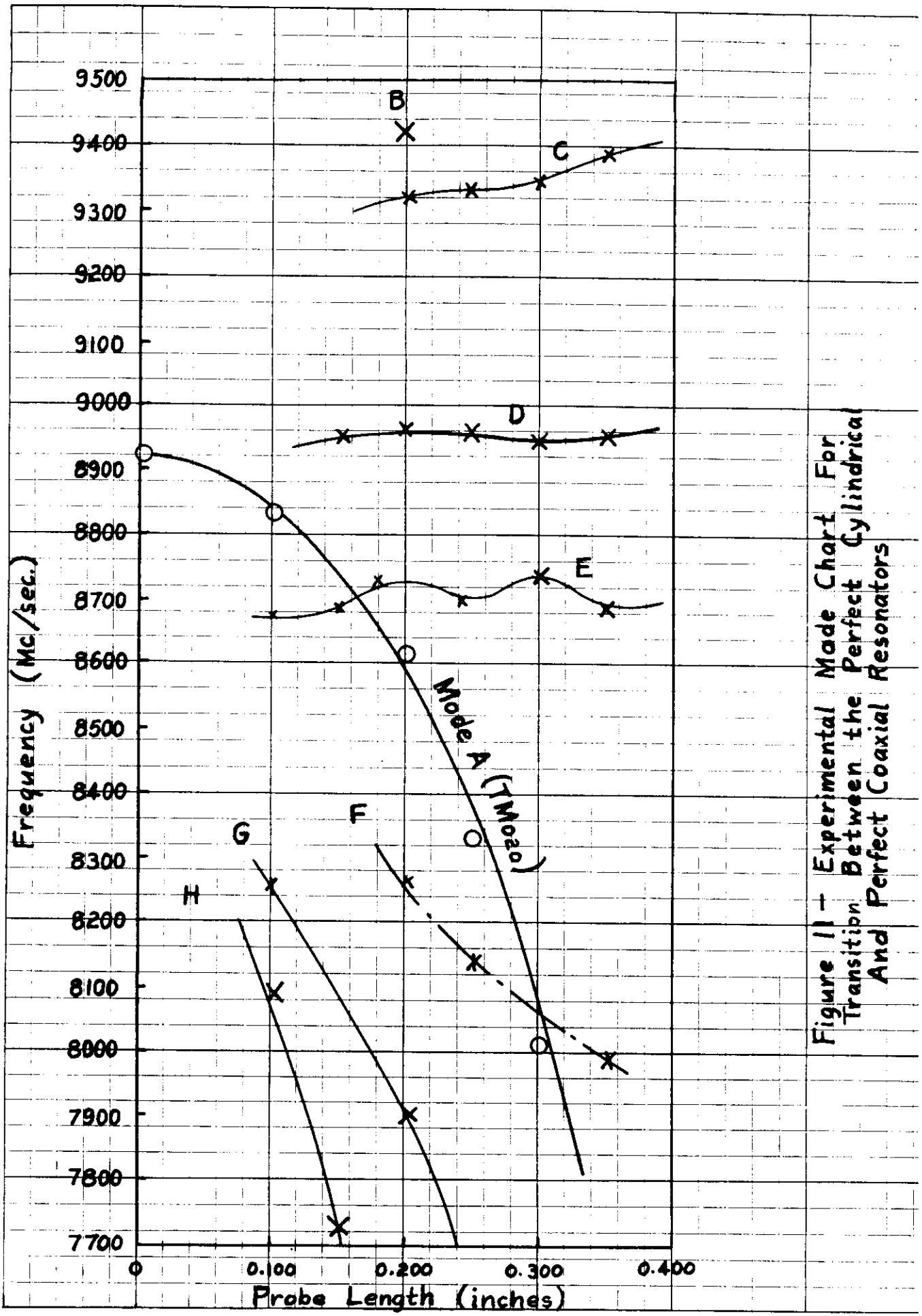

Figure 11 – Experimental Made Chart For Transition Between the Perfect Cylindrical And Perfect Coaxial Resonators

IV. COAXIAL LINE TO LOOP COUPLING IN WAVEGUIDE

Examination of figure 7 shows that the impedance presented by the probe for $(\ell/\lambda) = 0.5$ is too high to couple power from the TM_{020} resonator to a waveguide or load and requires a transformer of some kind to transform the 2400 ohms impedance to approximately 500 ohms characteristic impedance of waveguide. It is apparent that an approximately quarter-wave length section of line will perform this function. Since a bead or stub support must be used to hold the probe and center conductor rigidly, a loop in waveguide supporting the probe would be a good mechanical construction, provided the right electrical characteristics can be obtained. It is more practical to obtain empirical data for a first analysis, because this case departs more severely, than the probe coupling cases previously considered, from the conditions for which Condon's equation for loop coupling in resonators was derived.

The experimental data for such a loop is plotted in figure 12. In the region investigated, three modes are found. Mode 1 has the highest VSWR and hence is potentially the best transformer for coupling from probe in resonator to waveguide. The position of the voltage minimum shows that Mode 1 could be the TE_{10} mode of waveguide. The position of the voltage minimum of Mode 3 is that for the case in

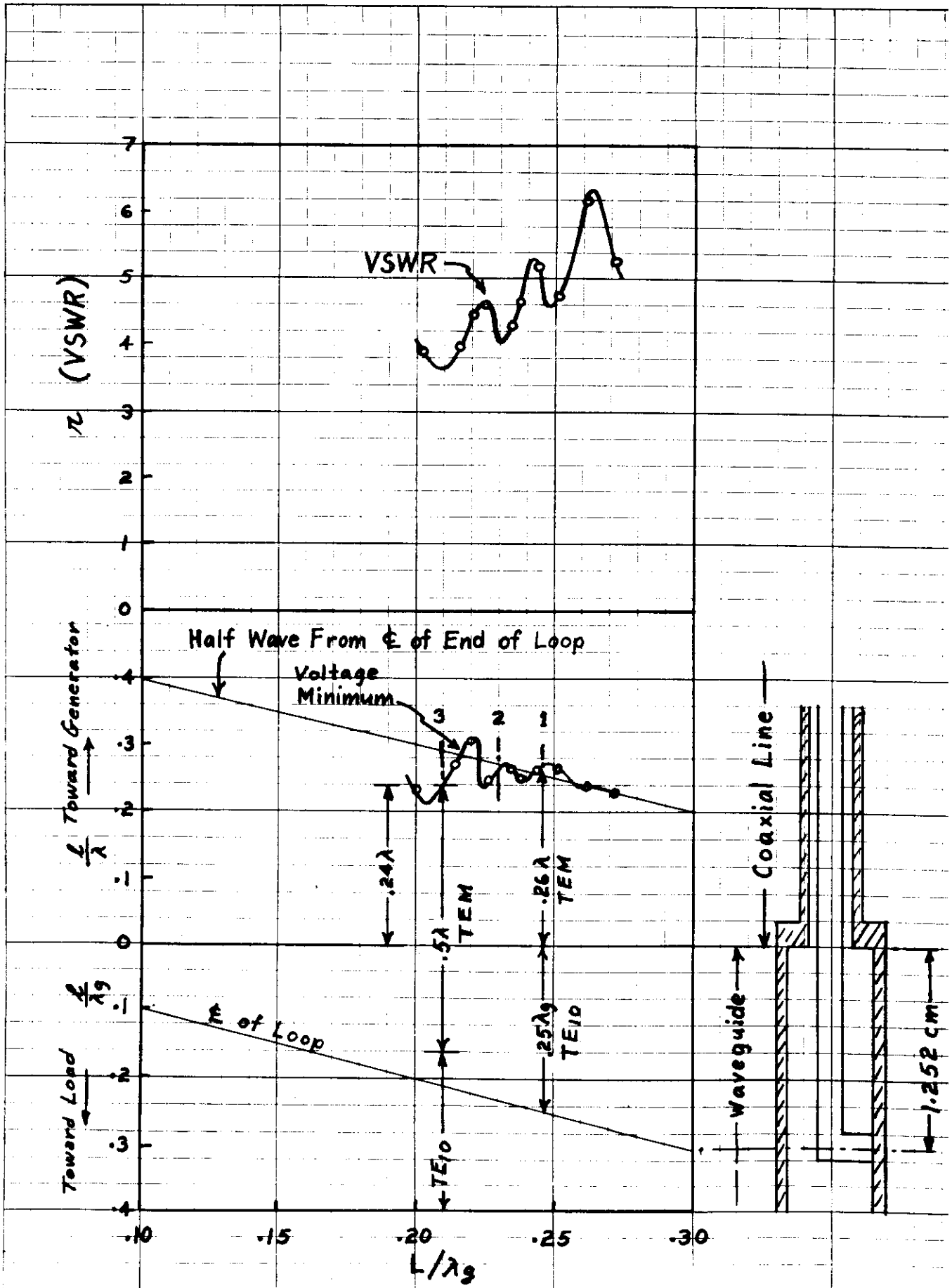

Figure 12— Experimental VSWR and Position of Voltage Minimun in Coaxial Line Coupled to Waveguide with Loop.

which the section of the waveguide containing the loop has the field distribution of a coaxial line, so that it could possibly be the TEM mode with a transition to the TE_{10} mode near the bend in the loop. Mode 2 has not been identified.

The usefulness of extrapolating Condon's equation for small loop coupling in high Q resonators to this case of large loop coupling to a waveguide terminated in its characteristic impedance is doubtful, so an outline of the procedure and difficulties encountered are as follows. Condon's[2] equation for the impedance of a loop in a resonator is as follows:

$$Z = R + \sum \frac{2\pi i f m_a^2}{\frac{\pi V}{c^2}\left(f_a^2 - f^2 + i\frac{f f_a}{Q_a}\right)} \qquad \begin{matrix}(19)\\ \text{c.g.s.}\end{matrix}$$

To use equation (19) a boundary for the rectangular resonator must be established. One method is to define the first half wavelength of the waveguide as a rectangular resonator coupled to an infinitely long waveguide through an iris equal to the full cross-section of the resonator and waveguide. For such a resonator the first term of the series at resonance reduces to:

$$Z_a = R + 9\times10^9 \frac{2bQ_{12}}{adf_a} \text{ ohms} \qquad \begin{matrix}(20)\\ \text{M.K.S.}\end{matrix}$$

Where Q_{L2} is determined by:

$$\frac{1}{Q_{L2}} = \frac{1}{Q_u} + \frac{1}{Q_{c2}}$$

Q_u from Skinnery[3] for TE_{101} mode, brass, frequency of 9070 mc./sec.

$$Q_u = \frac{\pi \eta_1}{4K_s} \left(\frac{(a^2+d^2)^{3/2}}{a^3+d^3+\frac{ad}{2b}(a^2+d^2)} \right) = 3935 \qquad (21)$$

A rough approximation of the coupled Q can be obtained by assuming that the energy stored in the resonator is equally divided between the wave traveling to the right and the wave traveling to the left. Since the right wave goes out the iris, one half the energy stored is lost and a coupled Q of 2 results from the following definition.

$$Q_{c2} = \frac{\pi \times \text{Energy stored in circuit}}{\text{Energy coupled out per half cycle}} = \frac{\pi U}{1/2\ U} = 2\pi \qquad (22)$$

Since this application of the definition of Q is not rigorous, the use of Q_{L2} from equation (22) in (20) would not be a valid test of the usefulness of equation (19). Moreover, the low Q would make the computation of many terms of the series necessary to get convergence. In this case the experimental data is used in designing the next part without a precise check against the theory.

V. LOOP IN WAVEGUIDE TO PROBE COUPLING IN THE TM_{020} MODE CYLINDRICAL RESONATOR

The problem of coupling power from a resonant circuit to a waveguide is the transformation of the impedance of the resonator of Section III by means of the data on loops in Section IV to a suitable value for matching out to a waveguide.

From figure 13 for $\left(\frac{\ell}{h}\right) = 0.500$ the voltage standing wave ratio (γ) as seen from a 50 ohm coaxial line is 48. From figure 12 the γ of a 1.252 centimeter length loop is 4.6. If the probe and loop are joined at the points at which they both appear as series resonant circuits, the loop will act as a transformer with an impedance ratio of 4.6. The theoretical γ in the waveguide should be approximately 48/4.6 = 10.4. The experimental γ from a circle 1 of figure 13 is 11, which is reasonably close to 10.4.

The inductive reactance of the loop contributes to the increase of the resonant frequency from 8617 mc. to 8672 mc. A comparison of the two circles of figure 13 is tabulated below:

Case A		Case B	
Probe from coaxial line.		Probe from loop in waveguide.	
f_o	= 8617	f_o	= 8672
ω_{L12}	= 16.3	ω_{L12}	= 46.2
γ_1	= 48	γ_1	= 11
ω_{12}	= 800	ω_{12}	= 576
Q_{c1}	= 16.7	ω_{c1}	= 52.4
β_1	$= \frac{\omega_u}{\omega_{c1}} = \frac{3750}{16.7} = 225$	β_1	$= \frac{\omega_u}{\omega_{c1}} = \frac{3750}{52.4} = 71.6$

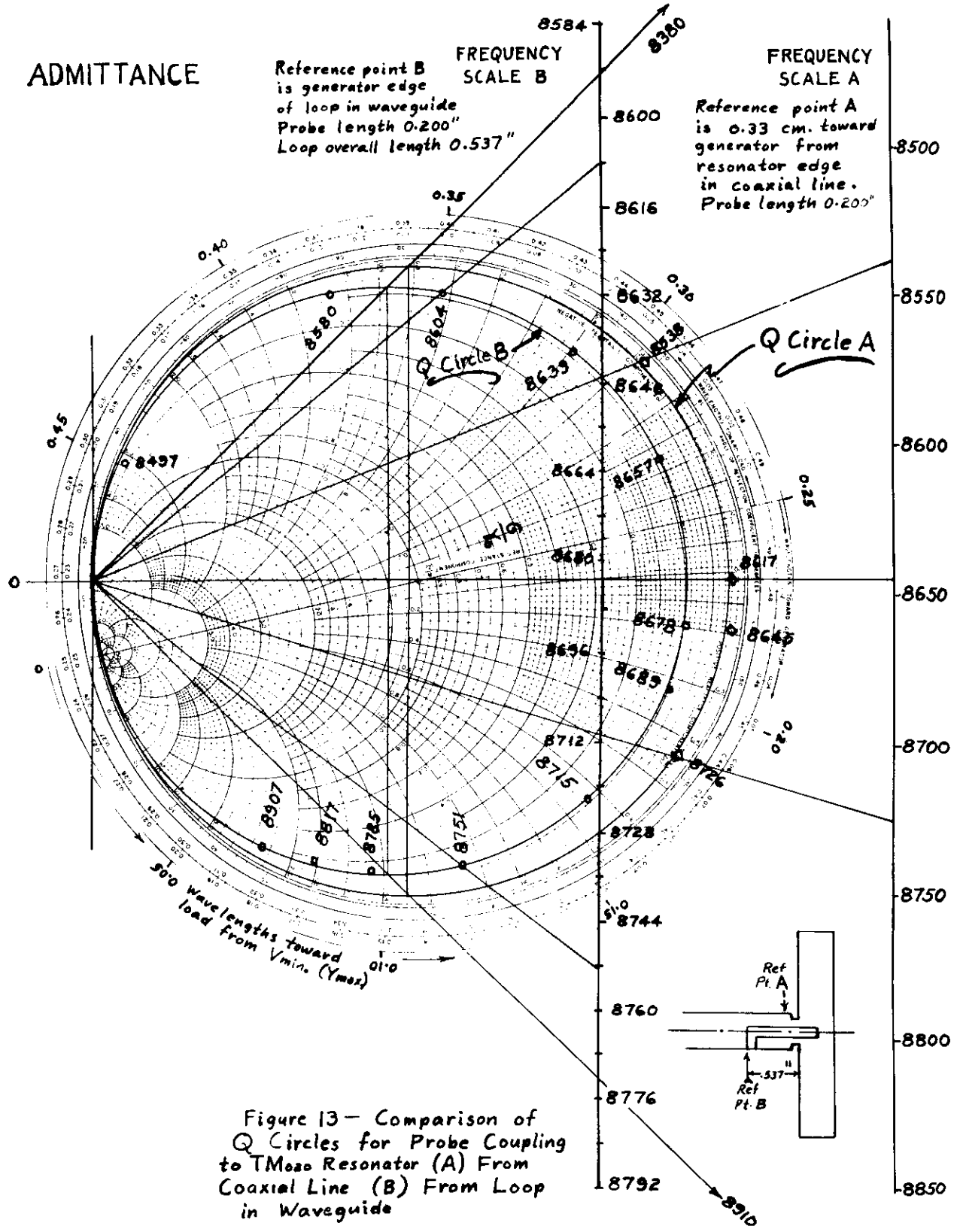

Figure 13 — Comparison of Q Circles for Probe Coupling to TM_{020} Resonator (A) From Coaxial Line (B) From Loop in Waveguide

To couple maximum power out of the resonator through the loop-probe, the VSWR presented to the electron beam (or in this case the waveguide connected to the loading iris) must be made unity. Using the terminology of Jaynes[4] where γ_2 is the VSWR at the input iris with the loop probe serving as the output, and β_1 and β_2 are the ratios Q_u/Q_{e1} and Q_u/Q_{e2} respectively, we have the equation:

$$\gamma_2 = \frac{\beta_2}{1 + \beta_1} \tag{23}$$

Then for $\gamma_2 = 1$; $\beta_2 = 1 + \beta_1$ (24)

For this condition of maximum output the input Q_e's would have to be as follows:

Case A	Case B
$Q_{e2} = 16.6$	$Q_{e2} = 31.7$

This means that for a given probe length the loop in waveguide method makes it possible to match the input for a higher loaded Q.

To transfer these results to the case where an actual electron beam is used, it is necessary to know the beam impedance. Equation (24) can still be used, since $\beta_2 = R_{sh}/R_{beam}$ where R_{sh} is the shunt impedance of the resonator at the place where the electron beam pass through the resonator.

It should be noted that when 1/2" and 1/4" iris widths are used together, q_{12} is found to have three different values.

Chapter II, D	$q_{112} = 241$
Chapter V, Case B	$q_{12} = 376$
Chapter V, Case A	$q_{12} = 800$

The irises are placed at points of maximum current density. The insertion of the probe distorts the field so that the maximum current region is shifted away from the irises, thus changing the coupling to the irises. This means that the procedure of breaking a microwave system into component parts is correct only if the changes considered in one component do not change the fields in the other components. However, even in such cases this method can be used to get reasonably good approximations.

VI. CONCLUSIONS

The addition of a half-wave shorted coaxial line of low characteristic impedance to a cylindrical TM_{020} mode resonator having a radius equal to the outer radius of the coaxial line reduces the unloaded Q in the ratio given by equation (2).

$$\frac{Q'_u}{Q_u} = \frac{a + b}{a + b + s} \tag{2}$$

For a small perturbation of a resonator wall at a point where E << H or E >> H the accurate formula for the frequency shift can be replaced by the approximation of equation (4).

$$\left(\frac{\omega}{\omega_a}\right)^2 = 1 \pm \frac{v}{v_o} \tag{4'}$$

The sign is plus for E << H and wall pushed in or E >> H and wall pushed in, and minus for E << H and wall pushed out or E >> H and wall pushed in.

When a resonator has several coupling devices associated with it such as one probe and two irises, the resonator with each coupling device can be treated separately and the results combined by use of equivalent circuits provided that each coupling device does not cause a serious change in the field at the other coupling devices. The loaded Q is measured for iris couplings to the resonator for use later on in the

study of probe coupling. When the probe length is extended to half the resonator height, a Q_{L12} of 240 is changed to 800. Even though the use of equivalent circuits becomes inaccurate for Q_{L12}, the method works for calculating the resonant impedance.

The resonant impedance at a probe in a TM_{020} cylindrical resonator can be approximated by equation (12) in which only the principal terms of Condon's equation are retained.

$$Z = R + jX = \frac{36 \times 10^9 \; h \; c}{\omega_a \; a^2 \; J_1^2(k_c a)} \left(\frac{l}{h}\right)^2 - j \frac{1}{\omega C} \quad \text{ohms} \qquad (12)$$
M.K.S.

The equation gives an R that is too high. For $\frac{l}{h} = 0.5$, R must be reduced by 38%.

The change in resonant frequency due to insertion of a probe in a cylindrical TM_{020} resonator can be accurately calculated by considering the probe as part of the resonator wall and then treating the system as a radial line with an equivalent discontinuity capacitance at the probe radius.

The insertion of a long probe in a cylindrical resonator can cause more undesired modes to appear than can be found nearby on a mode chart for perfect cylindrical resonators. The presence of additional modes is explained by change of the equivalent height of the resonator from a half-wave length to a quarter-wave length as the probe length is changed from zero to almost the full height.

When a coaxial line is coupled to a waveguide by a rectangular loop of approximately quarter-wave length, there is a resonance for the frequency at which the developed loop length is $\lambda_g/4$ for the TE_{10} mode in waveguide. There is also a resonance near the frequency for which the loop length is $\lambda/4$ in which the field probably approaches that for the TEM mode, so that the section of waveguide around the loop can be considered as an extension of the coaxial line. Another mode is found in between, which can probably be identified by calculating a sufficient number of terms in Condon's equation for loop for loop coupling.

The design of loop-in-waveguide to probe-in resonator coupling devices can be done on a practical basis by treating the resonator and probe as a series resonant circuit, to be connected to another series resonant circuit, a loop in waveguide. If the beam impedance of a resnatron anode resonator is known, then the desired cold impedance can be calculated for maximum power output.

VII. APPENDICES

A. Experimental Procedure

The test equipment is shown in figure 14. A 723A/B tube using a TVH-7BL Power Supply is the basic signal source. The signal is monitored for frequency and spectrum, by taking a small signal from a CG-176/AP Directional Coupler to a TSX-48B Spectrum Analyzer. In the early part of the work, standing wave ratios were measured by square wave modulating the 723A/B with the modulator contained in the TVH-7BL Power Supply. The signal picked up by the probe in waveguide or coaxial line was rectified by a 1N23B crystal and amplified by a TAA-161A Amplifier.

It was difficult to measure high standing wave ratios, because frequency modulation side bands due to slope of the modulation signal caused errors when the modulation was increased and amplifier gain increased. Although the signal could be observed with the spectrum analyzer and adjusted to eliminate troublesome sidebands, it was found to be more effective to use c-w and modulate the rectified output of the crystal by using a Perkin-Elmer d-c Breaker Amplifier.

A TPX-270M/25 Attenuator was used to isolate the 723A/B from the impedance being measured and to match the generator end of the slotted section. For measurements of waveguide admittance, a TPX-670M/YR Slotted Section and Probe was used.

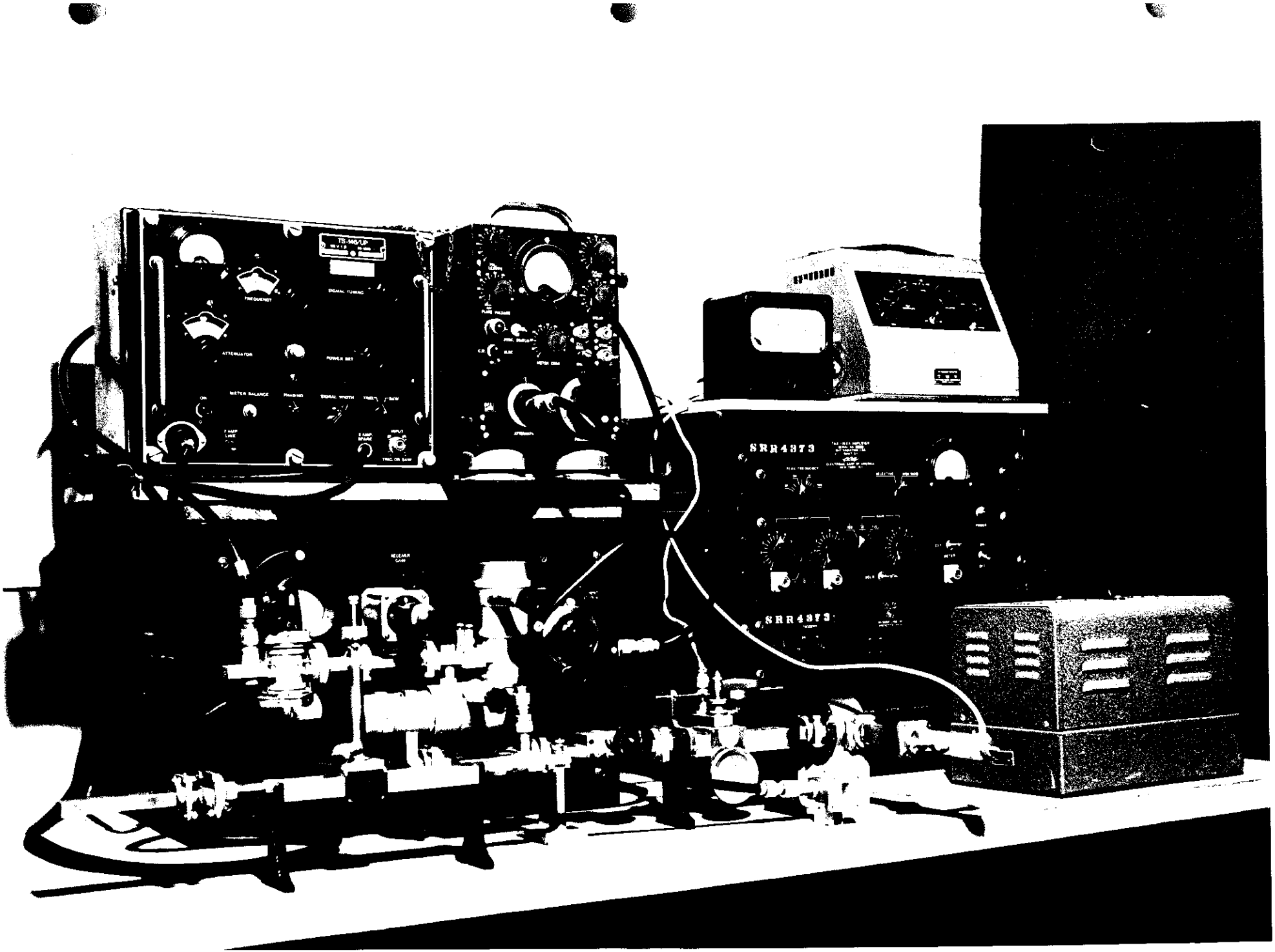
SRR4373
SRR4373

A dial gauge reading in 0.01 millimeters was added in order to measure VSWR's of the order of magnitude of one hundred by observing the shape of the standing wave pattern at the voltage minimum.

For measurement of coaxial impedance a TPS-60FH Slotted Section and Probe was used. Although designed for 3000 mc. it can be used all right at 9000 mc. The only error introduced is an uncertainty in the true position of the voltage minimum due to the failure of the adapter from cable to rigid coaxial line to be a perfect match. The VSWR of the adapter is not greater than 3.0, so the reflection coefficient Γ_0 is less than 0.51. The phase angle error introduced is less than θ, where $\sin. \theta = \Gamma_0 \Gamma_1$. The maximum possible error in phase is $.085 \lambda$. This can make the position of the voltage minimum in error in figures 7, 12 and 13(a). This error need not affect the design of loops and probes, if care is taken to place all objects being measured at equivalent distances from the slotted section so that errors in phase will approximately cancel out.

A TPX-340M Flap Attenuator was placed between the output iris of the resonator and the TPX-360M Crystal Mount to keep the impedance presented to the iris equal to the characteristic impedance of the waveguide.

For frequency measurements outside the range of the Spectrum Analyzer, the wavelength in the coaxial slotted

section or the guide wavelength in the waveguide slotted section was measured. The slotted sections were not accurate enough for the measurement of small frequency differences, so an extra 723A/B tube using a TS-146/UP Test Set as a power supply was added to the spectrum analyzer. A 550 to 1300 mc. signal from an LAV-2 Signal Generator was coupled through a 1N21 crystal in the auxiliary tube mount to supply beat frequencies outside the ordinary spectrum analyzer range. Small frequency differences were read by tracking the beat frequency with the signal generator signal on the spectrum analyzer oscilloscope, observing the frequencies on the LAV-2 dial.

Since the load end of the TS-68/U coaxial slotted section is supported by the load and the probe has no support, it was necessary to insert a polystyrene bead for support and then transform the observed data to the load side of the bead by use of a Smith chart slide rule.

Descriptions or references to the appropriate microwave testing techniques can be found in Volume 11 of the M.I.T. Radiation Laboratory Series.[14]

B. λ_g and Frequency of Cylindrical Resonator

For a perfect $TM_{0\ell 0}$ resonator the fields in the resonator correspond to those given by Hamo and Whinnery[3] for a $TM_{\ell 10}$ resonator.

$$E_z = E_0 J_0 (k_0 r)$$

$$H_\phi = j \frac{E_0}{\eta_1} J_1 (k_0 r) \qquad (25)$$

$$k_0 = \frac{2\pi}{\lambda} = \frac{p\,2}{a} = \frac{5.52}{a}$$

Energy Stored:

$$U_E = h \int_0^a \frac{\epsilon_1 |E|^2}{2} 2\pi r\, dr = \pi \epsilon_1 h E_0^2 \frac{a^2}{2} J_1^2(k_0 a) \qquad (26)$$

Power lost in walls:

$$P_L = \frac{\pi a R_s E_0^2}{\eta_1^2} J_1^2(k_0 a) \left[h + a\right] \qquad (27)$$

Unloaded Q for perfect cylinder:

$$Q_u = \frac{\omega U_E}{P_L} = \frac{\eta_1}{R_s} \frac{p_{02}}{2} \frac{1}{1 + \frac{a}{h}} \qquad (28)$$

The addition of the half-wave coaxial section is treated as follows: Let I_0 be current density at end of coaxial line. The $I_0 = H_\phi$ for $r = a$. The current density at distance x from the end is I_x.

$$I_x = I_0 \cos \frac{2\pi x}{\lambda_1}$$

I_e = effective current

I_t = total peak current $I_t = 2\pi a\ I_x$

P_c = power lost in walls of coaxial section

$$P_c = I_c^2 \frac{2s R_2}{2\pi a} = \frac{I_{ax}^2}{2} \frac{s R_s}{\pi a} \tag{29}$$

I_{ax} = average of peak current with respect to x.

$$I_{ax}^2 = \frac{1}{\pi} \int_{x=0}^{x=s} I_t^2 \, d(k_c x) = \frac{4\pi^2 a^2 I_0^2}{\pi} \int_0^{\pi} \cos^2 (k_c x) \, d(k_c x) =$$

$$= 2\pi^2 a^2 I_0^2 \tag{30}$$

Then by (25), (29), (30)

$$P_c = I_0^2 \pi a s R_s = \frac{\pi a R_s k_0^2}{\eta_1^2} J_1^2(k_c a) \, [s] \tag{31}$$

$$Q_l' = \frac{\omega W_E}{P_L + P_c} = \frac{\eta_1}{R_s} \frac{P_{02}}{2} \frac{h}{h+a+s} \tag{32}$$

By (28) and (31) $$\frac{Q_l'}{Q_l} = \frac{a+h}{a+h+s} \tag{33}$$

Correction for Pushed Out Walls

Since Slater's formula is for pushed in walls ($-dv$) must be substituted for (dv) for the case of pushed out walls. The H_a's are normalised so.

$$\int_V H_a \cdot H_b \, dv = \begin{cases} 1 & \text{for } a = b \\ 0 & \text{for } a \neq b \end{cases}$$

For the TM_{020} cylindrical resonator:

$$\int_V H_a \cdot H_b \, dv = \int_0^a \frac{k_0^2}{\eta_1^2} J_1^2(k_c r) \, h \, 2\pi r \, dr = \frac{a^2 k_0^2 \pi h}{\eta_1^2} J_1^2(k_c a) = 1$$

This determines the numerical value of E_0.

$$E_0^2 = \frac{\eta_1^2}{a^2\pi h\, J_1^2(k_c a)} \qquad E_\beta^2(z) = \frac{E_0^2\, J_1^2(k_c a)}{\eta_1^2} = \frac{1}{a^2\pi h} \tag{34}$$

At the boundary E_a is zero and for small perturbations, it can be assumed zero throughout the volume of the perturbation. Also, for small perturbations, H_a can be assumed equal to its value at the boundary.

$$\left(\frac{\omega}{\omega_a}\right)^2 = 1 + \int (H_a^2 - 1_a^2)(-dv) = 1 - H_a^2 \int dv = 1 - \frac{V}{a^2\pi h} =$$

$$= 1 - \frac{V}{V_0} \tag{35}$$

For the resonator of figure 3:

$$V = 0.8\ h \quad cm^3 \qquad V_0 = \pi a^2 h = 26.7\ h \quad cm^3$$

C. Impedance of Probe in TM_{020} Cylindrical Resonator

First it is noted that Gordon normalized the energy stored in each mode to the volume of the resonator, while Slater normalized to unity. The magnetic vector potential, A_a, in equation (11) is normalized as follows, using the treatment of TM-waves given by Schelkunoff.[15]

$$A_a = \frac{i\omega\epsilon}{\chi^2} E_{za} = i\, \frac{E_0 J_0(k_c r)}{\chi \eta} \tag{36}$$

M.K.S.

Using equations (11), (25), and (36):

$$\int A_a(r)\cdot A_a(r)\,dV = \int_0^a \frac{E_0^2 J_0^2(k_0 r)}{\chi^2\eta^2}\,2\pi r h\,dr =$$

$$= \frac{2\pi h E_0^2}{\chi^2\eta^2}\;\frac{a^2}{2}\,J_1^2(k_0 a) \qquad (37)$$

Equation (37) is in M.K.S. units while Condon used c.g.s. units. In following equations, the whole integral of equation (37) is carried through until there is no possibility of mixing up the different units.

The first term of the series of equation (9) is simplified at resonance and by use of (37) (1), (36)

$$E_a = \int_0^{\ell} A \cdot ds = \frac{E_0 J_0(0)\, h}{\chi\eta}\left(\frac{\ell}{h}\right)$$

ℓ = length of probe

$$R = 10^{-9}\,\frac{2\pi i\, r\, E_a^2}{\left[\frac{\pi}{a^2}\int A\cdot A\,dV\right]\left(i\,\frac{r^2}{\omega_a}\right)} =$$

$$= 10^{-9}\;\frac{2a^2\omega}{r}\;\frac{\ell^2}{\pi h a^2 J_1^2(k_0 a)} \text{ ohms} \qquad \text{c.g.s.}$$

$$R = \frac{36\times 10^9\,\ell^2\,\omega}{\omega_a\, h\, a^2\, J_1^2(k_0 a)} \text{ ohms} \qquad (36)\ \text{M.K.S.}$$

D. Correspondence of Probe Impedance and Shunt Impedance of Resonator

R_{sh} is the shunt impedance of a TM_{020} resonator at the center.

$$R_{sh} = \frac{(E_0 h)^2}{2 P_L} \qquad (39)$$

From (28) $$P_L = \frac{\omega W_E}{Q} \quad \text{then} \quad R_{sh} = \frac{E_0^2 h^2 Q}{\omega W_E}$$

By (26) $$R_{sh} = \frac{\left(\frac{1}{\pi \epsilon_1}\right) h^2 Q}{\omega_a h a^2 J_1^2(k_c a)} \qquad \epsilon_1 = \frac{1}{36\pi \times 10^9}$$

$$R_{sh} = \frac{36 \times 10^9 \, h^2 Q}{\omega_a \, h \, a^2 \, J_1^2(k_c a)} \qquad (40)$$

M.K.S.

If ℓ^2 is substituted for the h^2 in the numerator of equation (40), the result is equation (36). This means that when the probe goes all the way across the resonator, the impedance at the probe is the full shunt impedance of the resonator, if the fields are not seriously distorted by the probe.

VIII. BIBLIOGRAPHY

1. Frederick B. Wood, The History of Electromagnetic Theory, (E. E. Seminar Paper), Berkeley (1947).

Section II on microwave waveguide transmission lists the basic references on cavity resonators.

2. E. U. Condon, "Forced Oscillations in Cavity Resonator," J.A.P., 12, p. 129-132, Feb. 1941.

Equations for impedance of loop and probe coupling to resonator.

3. S. Ramo and J. R. Whinnery, Fields and Waves in Modern Radio, N.Y. Wiley (1944).

Radial transmission lines, pp. 364-460
Foreshortened radial lines, pp. 406-408
Transition between coaxial and radial resonators, pp. 408-410
TM_{010} Mode in cylindrical resonator, pp. 396-399

4. E. T. Jaynes, Theory of Microwave Coupling Systems, Washington, D.C.: Combined Research Group, Naval Research Laboratory, CRG Report 84, Aug. 29, 1945.

5. J. C. Slater, "Microwave Electronics," Rev. Mod. Phys., Vol. 18, pp. 441-512, Oct. 1946.

Resonant Cavities, pp. 457-469
Input Impedance, pp. 476-480
Perturbation of Boundary, pp. 482-483
Tuning of Resonant Cavity, pp. 483-485
Measurement of Cavity Resonance, pp. 486-489

6. H. A. Bethe, R. E. Marshak, and J. Schwinger, Theoretical Results on the T-R Box, Cornell University, NDRC Report 14-114, Jan. 20, 1943.

Includes iris and loop coupling analysis for TR box.

7. L. B. Smullen and Carol G. Montgomery, Microwave Duplexers, N.Y.: McGraw-Hill Book Co. (1948).

Chap. 2. Linear Theory of High-Q TR Tubes includes material on iris and loop coupling.

8. E. O. Willoughby, "Some Applications of Field Plotting," Jour. I.E.E. (London), part III, 93, pp. 275-292, July 1946

and

P. D. Crout, "A Flux Plotting Method for Obtaining Fields Satisfying Maxwell's Equation, With Application to the Magnetron," J.A.P., 18, pp. 348-355, April 1947 (MIT RL Rpt 1048).

9. Karl Spangenberg and Glenn Walters, "An Electrical Network for the Study of Electromagnetic Fields," Technical Report No. 1, May 15, 1947, ONR Contract N6-ori-106 Task III.

10. J. R. Whinnery and H. W. Jamieson, "Equivalent Circuits for Discontinuities in Transmission Lines," Proc. I.R.E., Vol. 32, pp. 98-114, Feb. 1944.

11. Unpublished paper by J. R. Whinnery and T. F. Robbins on Radial Line Discontinuities.

12. I. G. Wilson, C. W. Schramm and J. P. Kinzer, "High Q Resonant Cavities for Microwave Testing," B.S.T.J., XXV, pp. 408-434, July, 1946.

Field equations, wavelength, Q, mode charts for cylindrical resonators, tables of Bessel function zeros for first 180 modes in cylindrical resonators.
Note: Some information from Kinzer, especially coaxial modes, not contained in the above article, is published in: C. B. Montgomery, Techniques of Microwave Measurements, N.Y.: McGraw-Hill BookCo., (1947), pp. 294-307. (MIT Radiation Laboratory Series, Volume 11).

13. W. L. Barrow and W. W. Mieher, "Natural Oscillations of Electrical Cavity Resonators," Proc. I.R.E., Vol. 28, pp. 184-191, April 1940.

14. Carol S. Montgomery, Techniques of Microwave Measurements, N.Y.: McGraw-Hill Book Co. (1947).

15. S. A. Schelkunoff, Electromagnetic Waves, N.Y.: Van Nostrand Co. (1943).

Transverse magnetic plane waves, pp. 375-379.